Characterization of borosilicate microchannel plates functionalized by atomic layer deposition

C. Ertley*[a], O. H. W. Siegmund[a], J. Schwarz[a], A. U. Mane[b], M. J. Minot[c], A. O'Mahony[c], C. A. Craven[c], M. Popecki[c]

[a]Experimental Astrophysics Group, Space Sciences Laboratory, 7 Gauss Way, University of California, Berkeley, CA 94720

[b]Argonne National Laboratory, 9700 S. Cass Avenue, Argonne, IL 60439

[c]Incom, Inc. 294 Southbridge Road, Charlton, MA 01507

ABSTRACT

Borosilicate microcapillary arrays have been functionalized by Atomic Layer Deposition (ALD) of resistive and secondary emissive layers to produce robust microchannel plates (MCPs) with improved performance characteristics over traditional MCPs. These techniques produce MCP's with enhanced stability and lifetime, low background rates, and low levels of adsorbed gas. Using ALD to functionalize the substrate decouples the two and provides the opportunity to explore many new materials. The borosilicate substrates have many advantages over traditional lead glass MCPs, including the ability to be fabricated in large areas (currently at 400 cm^2).

Keywords: Microchannel Plate, Imaging, Photon Counting, Atomic Layer Deposition

1. INTRODUCTION

Microchannel plates (MCPs) are widely used in many scientific and technical applications[1-9]. The operational parameters of MCPs, wide gain range (10^2 - 10^8), fast response time (< 1ns), high spatial resolution (on the order of the pore diameter), radiation hardness, low intrinsic background, large area formats and no need for cooling, make them an ideal imaging scheme. Open-faced detectors or ultra high vacuum-sealed tube devices in conjunction with detection efficiency enhancing photocathodes are used in the detection of charged particles, photons, and neutrons[9].

Our research group, in collaboration with other Universities, National Laboratories, and Industry, is actively pursuing several MCP performance areas that can be improved upon. A program has been initiated which utilizes MCPs constructed by atomic layer deposition (ALD) on borosilicate microcapillary arrays to develop a Large Area Picosecond Detector[10]. The MCP construction begins with inexpensive hollow borosilicate tubes, which are drawn and assembled into a microcapillary array. Unlike traditional MCPs, it is not necessary to remove a core glass after the array is fused together. Resistive layer and secondary emissive layer deposition using the ALD process[11] replaces the hydrogen reduction used for conventional MCP activation. After functionalization of the MCP is complete, a final contact electrode can be applied. The steps in this process have been decoupled allowing for the operational parameters, such as resistance, to be adjusted independently. The borosilicate substrates have a high glass softening temperature (>700 ºC) opening the doors for many high temperature enhancement processes to be subsequently accommodated. Using borosilicate substrates with ALD functionalization significantly reduces MCP outgassing[12], which may have a direct effect on MCP detector lifetimes. Another advantage is the low intrinsic radioactivity of the borosilicate glass (low ^{40}K content) resulting in lower backgrounds than conventional MCPs[12,13].

Incom Inc. have fabricated a wide range of high quality borosilicate microcapillary substrates for use as MCPs (Fig. 1). The substrates have pore sizes ranging from 10 µm – 40 µm, bias angles of 8º, and pore length to diameter ratios of 80:1, 60:1, and 40:1. Substrates have been fabricated in several sizes ranging from 25 mm circular to 200 mm square and can have open area fractions from 55% to 83%. A new generation of borosilicate glass is now being used to further improve over the performance behaviors found in previous generations. Argonne National Laboratory has performed much of the current ALD functionalization, after which, the MCPs are sent to the University of California, Berkeley Space Science Laboratory for testing. Borosilicate MCPs with resistances from 5 MΩ to > 1 GΩ have been produced with secondary emissive layers of Al_2O_3 and MgO.

* camden.ertley@ssl.berkeley.edu; phone: 1 (510) 664-4699; fax: 1 (510) 643-9729; www.ssl.berkeley.edu/eag/

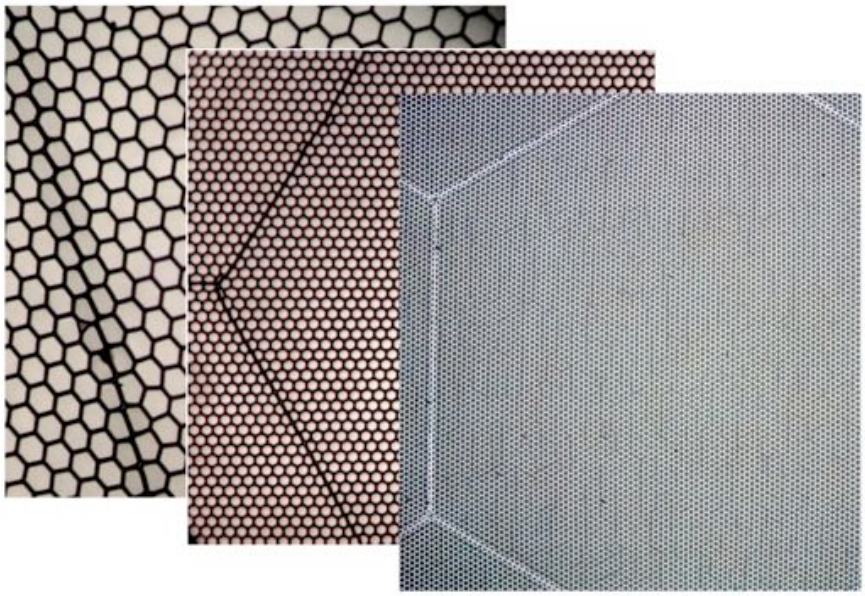

Fig. 1: Borosilicate micro-capillary substrates used for atomic layer deposited MCPs, left - 40 µm pores with 83% open area, middle - 20 µm pores, 65% open area, right - 10 µm pores, 55% open area.

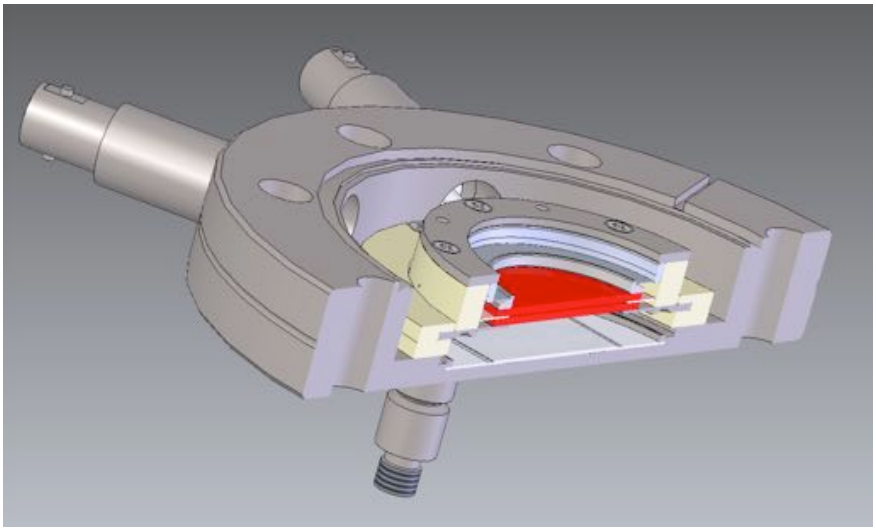

Fig. 2: Drawing of a 4.5" diameter detector flange used to evaluate the 33 mm MCPs. A gapped pair of MCPs (red) are clamped in the flange above a cross delay line anode (light gray).

2. ATOMIC LAYER MCP PERFORMANCE USING BOROSILICATE SUBSTRATES

Testing to date has concentrated on 33 mm diameter circular and 200 mm × 200 mm square substrates. The 33 mm substrates are a good medium to evaluate and optimize the ALD process. Evaluation of the general operational characteristics of the MCPs can be done with a basic set of tests. The MCPs are mounted in a detector flange above a cross delay line anode in either a two plate gapped configuration (Fig. 2) or a triple MCP "Z" stack. Testing begins with the evaluation of the MCP resistance by measuring the current–voltage characteristics. Once the resistance has been established, the absolute gain is determined by measuring the gain–voltage relationship. This is accomplished using a two MCP stack with a 0.7 mm inter–MCP gap biased at 200 V, the top plate is a standard MCP and the bottom plate is to

be tested. Using the top MCP as an electron source, the input current to the test MCP is established. The output current is measured for a known input current providing the gain as a function of the applied potential. Gain–voltage curves for the current generation of Al_2O_3 coated borosilicate MCPs are presented in Fig. 3 and are slightly improved compared to standard lead glass MCPs[7,14] and previous generations[15]. Testing of the MCPs continues with imaging the photon counting readout of a cross delay line anode. This setup provides imaging capabilities as well as a gain map of the MCP pair and pulse amplitude distributions. Using an input illumination of 185 nm UV light, the representative pulse amplitude distributions for a pair of Al_2O_3 coated borosilicate MCPs is shown in Fig. 4. The peaked distribution shows the photon signal detection and the negative exponential background distribution. The background events are attributed to radioactive decay of ^{40}K in the glass or to muon detection throughout the bulk of the MCP material. The pulse amplitude distributions shown in Fig. 4 agree with previous generations of ALD coated borosilicate MCPs and conventional MCPs in the same configuration[15].

The cross delay line detector[12] used to evaluate the event counting performance of the MCP pairs has a typical spatial resolution of <50 µm FWHM. The images, for example Fig. 7, show hexagonal modulation from the edges of the multi-fiber bundles, a product of the substrate manufacturing process. The modulation in the image is modest and the gain near the boundaries has been found to vary on the order of 5% to 10%. The background images show uniform event rates of 0.07 events cm^{-2} sec^{-1} for typical samples. This is lower than that measured with typical lead glass MCPs due to the lower ^{40}K content of the borosilicate glass.

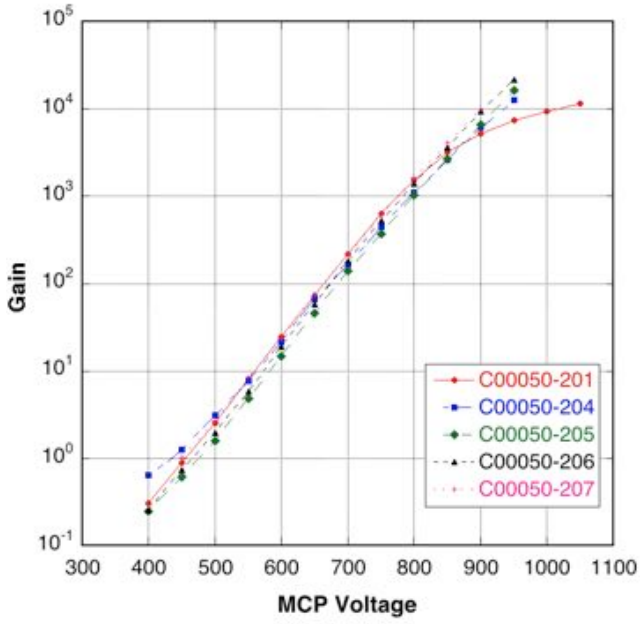

Fig. 3: Gain characteristics of 33 mm diameter Al_2O_3 coated borosilicate substrate, 20 µm pores, 70% open area, 60:1 L/D.

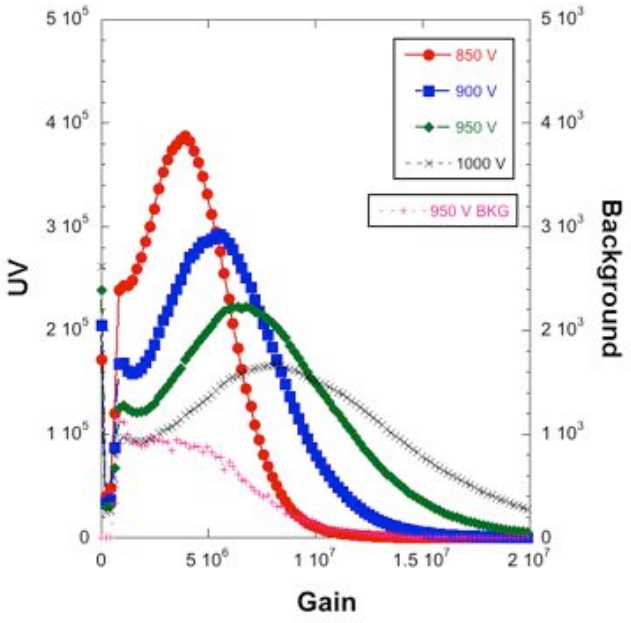

Fig. 4: Pulse amplitude distributions for a pair of 33 mm diameter Al_2O_3 coated borosilicate substrate, 20 µm pores, 70% open area, 60:1 L/D.

3. PERFORMANCE OF NEXT GENERATION ATOMIC LAYER MCP WITH BOROSILICATE SUBSTRATES

Next Generation Borosilicate ALD MCP Preconditioning and Lifetime Characteristics

The longevity and stability of borosilicate ALD MCPs was studied by preconditioning[16] the MCPs. The preconditioning is accomplished by illuminating with a uniform source of electrons from a standard MCP and setting the output current to ~1 µA to "burn in" the test MCP. Throughout the preconditioning, the "burn in" was periodically paused and a full function test was performed (gain–voltage, current–voltage, and imaging). The burn-in tests with this next generation substrate-MgO-ALD shows a modest gain increase followed by stabilization at about the initial gain (Fig. 5). The gain uniformity, even after ~1 C cm^{-2} of charge extracted, is quite good (Fig. 7). Burn-in tests on the next generation substrates coated with Al_2O_3 show a substantial decrease (~factor of 10) in gain followed by a small increase before

stabilizing (Fig. 6). These results agree with previous preconditioning tests with the first generation borosilicate ALD MCPs[15] with Al_2O_3. Standard MCPs require more charge extraction before gain stabilization is seen, reducing the preconditioning requirements of instruments, such as sealed tube devices, when using ALD MCPs.

Further testing of 33mm 20µm Al_2O_3 and MgO coated borosilicate substrate MCPs has proceeded and shows that these MCPs have extremely narrow (Fig. 8) pulse height distributions at low gain. This is critical to support low gain – high rate devices. High rate tests using low resistance MCPs shows good high rate gain stability, with supportable rates up to ~40 kHz in a 100 µm spot (Fig. 9).

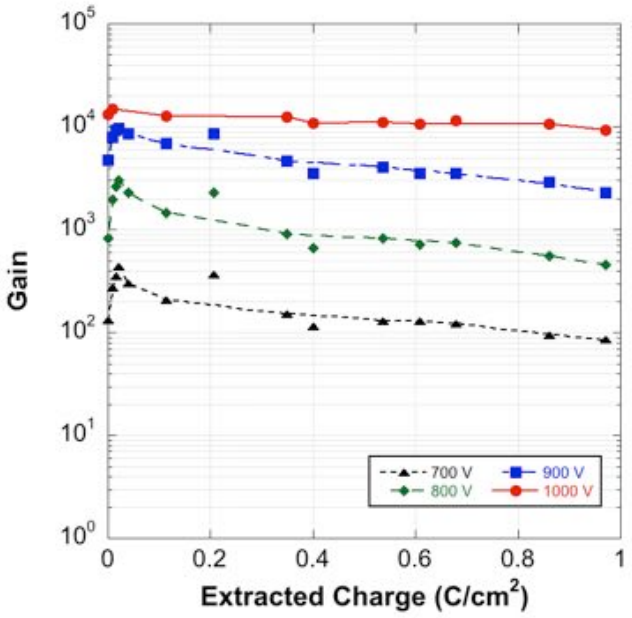

Fig. 5: Gain at specific bias voltages for a MgO coated borosilicate ALD MCP pair (20 µm pore, 60:1 L/d, 8° bias) as a function of extracted charge during UV burn-in.

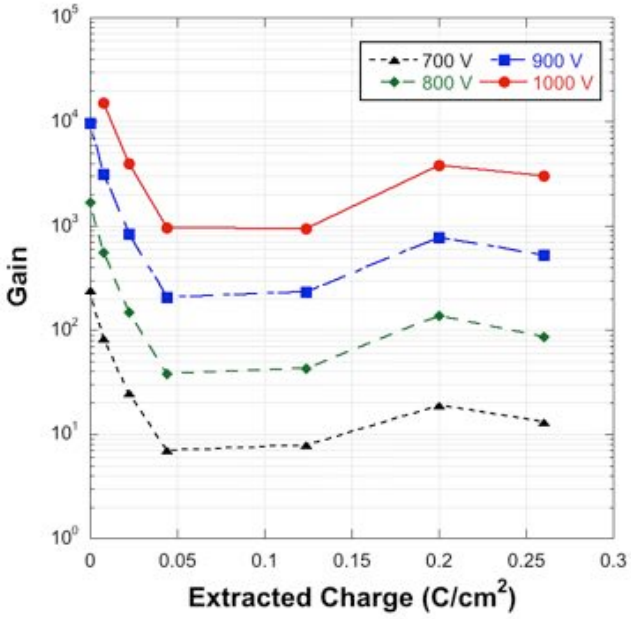

Fig. 6: Gain at specific bias voltages for an Al_2O_3 coated borosilicate ALD MCP pair (20 µm pore, 60:1 L/d, 8° bias) as a function of extracted charge during UV burn-in.

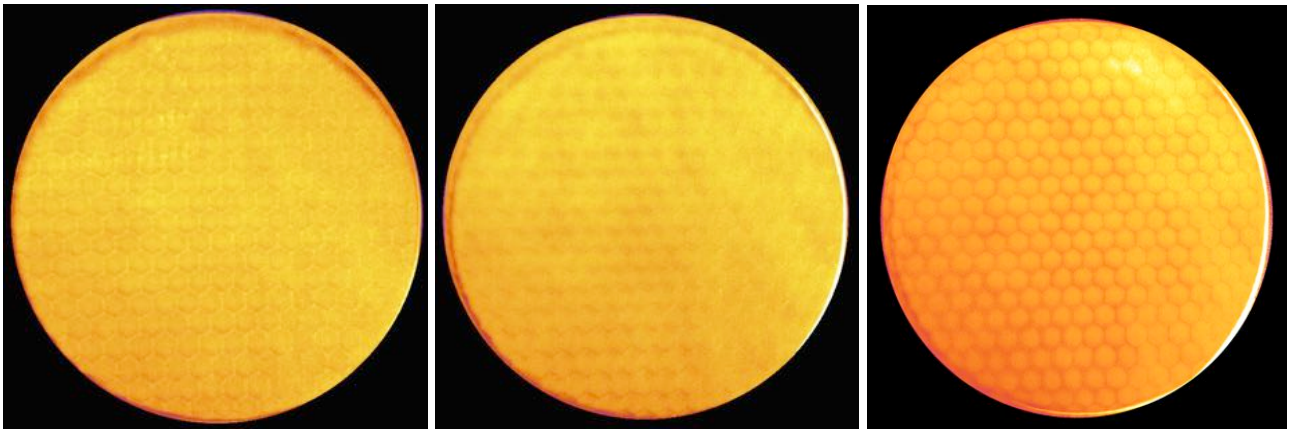

Fig. 7: Gain map of MgO coated borosilicates MCP at three stages of preconditioning, at 0.0 C/cm2, at 0.5 C/cm2, at 1.0 C/cm2. Substrate has 20 µm pores, 8º bias, and 60:1 L/d

Borosilicate ALD MCP Gamma & Beta Efficiency

A big advantage of borosilicate ALD MCPs over traditional MCPs is the lack of lead in the glass. We have tested the beta and gamma efficiency of both traditional MCPs and ALD MCPs using ^{90}Sr and ^{60}Co sources respectively. The beta

efficiency, at ~1.5 MeV, of standard MCPs is 48% and 43% for ALD MCPs. However, the efficiency of Gamma rays (~1MeV) is 3% for standard MCPs and 1.8% for ALD MCPs. Without lead in the glass, the gamma ray efficiency for borosilicate ALD MCPs is almost 2x lower. This can be further improved by applying an upper level threshold. This gives a Beta efficiency of 20% and a Gamma efficiency of 1.3% for ALD MCPs (see Fig. 10 & 11).

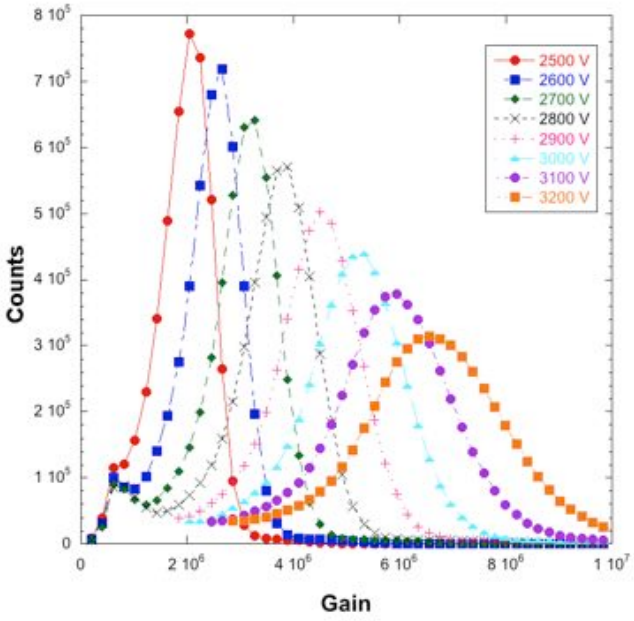

Fig. 8: Tight pulse amplitude for a 3 MCP stack of 33 mm diameter MgO coated borosilicate MCPs (60:1 L/D)

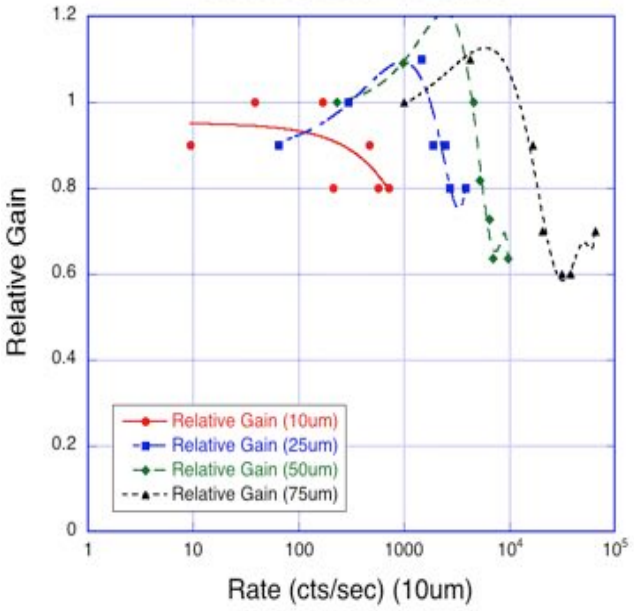

Fig. 9: High rate tests using low resistance MCPs shows good high rate gain stability, with supportable rates up to ~40 kHz in a 100 µm spot

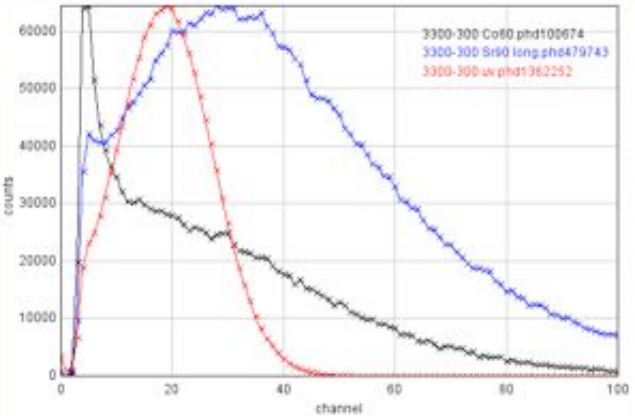

Fig. 10: Pulse amplitude distributions with a standard glass (Gain ~5 x 10^6) MCP for three different sources. ^{90}Sr Beta (blue), ^{60}Co (black), UV (red)

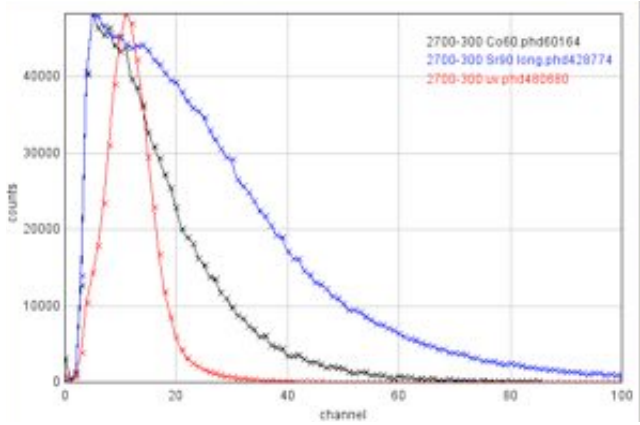

Fig. 11: Pulse amplitude distributions with a ALD + borosilicate glass (Gain ~3 x 10^6) MCP for three different sources. ^{90}Sr Beta (blue), ^{60}Co (black), UV (red)

Bare ALD-MCP Quantum Efficiency

Applying an electrode to a ALD MCP increase the detection efficiency for UV photons. By applying the electrode, the quantum efficiency (QE) of an ALD MCP becomes similar to that of a standard MCP (Fig. 12). The QE of the MCP is dependent on the incident angle of the light. The QE falls off at large angles and when the light is directed down the MCP pores (Fig. 13).

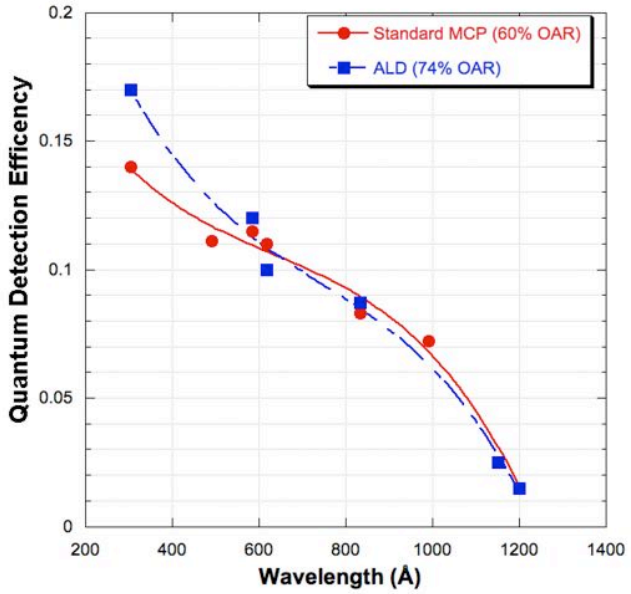

Fig. 12: BARE ALD – borosilicate MCP, photon counting quantum detection efficiency, normal NiCr electrode coating gives normal bare MCP QE.

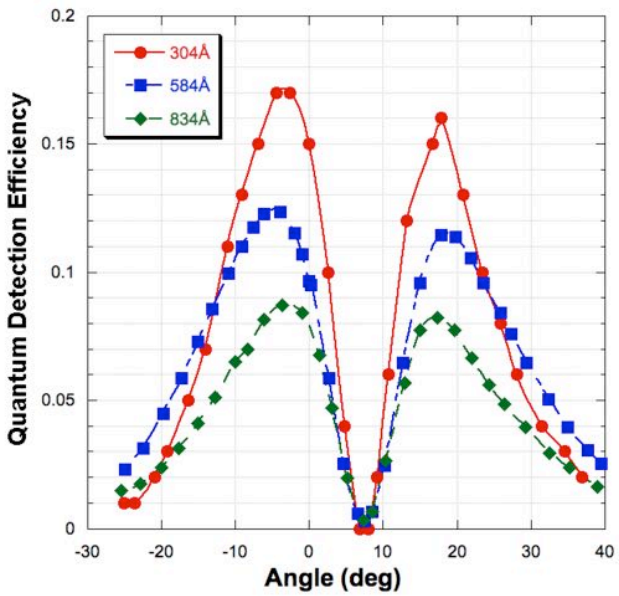

Fig. 13: Quantum efficiency vs the light incident angle for a bare ALD MCP. The QE falls off at large angles and when the light is pointed directly down the pore.

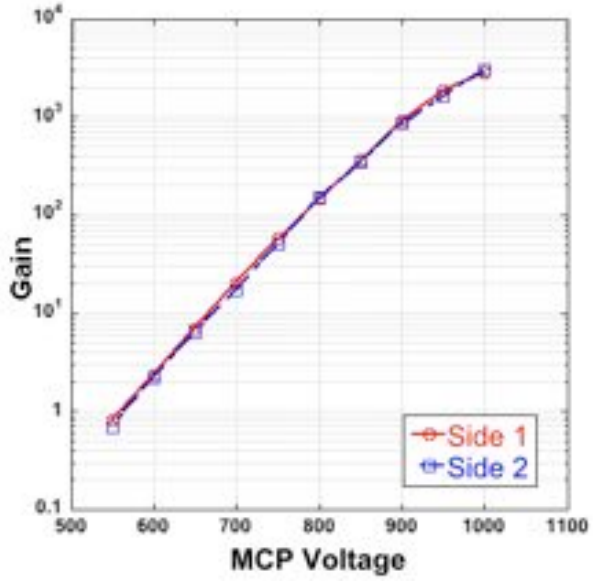

Fig. 14: Gain characteristics for a 20 cm MCP. Al_2O_3 ALD 20µm pore, 60:1 L/d borosilicate MCP. The gain is similar for both sides of the plate.

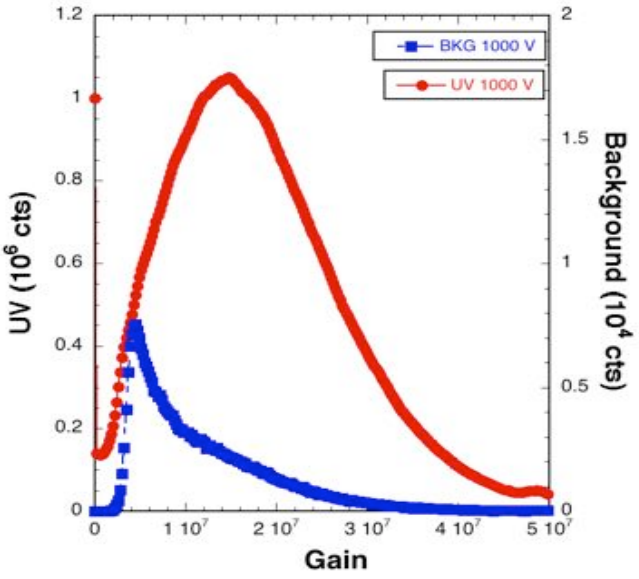

Fig. 15: The pulse amplitude distribution for a 20 cm MCP pair. Al_2O_3 ALD 20µm pore, 60:1 L/d borosilicate MCP, 185 nm illumination, 1000 V bias on each MCP.

20 cm Borosilicate Substrates, Atomic Layer MCPs

Borosilicate microcapillary substrates are more robust compared to standard MCP glass, which means the borosilicate substrates can be fabricated in larger areas. Borosilicate substrates with 20 µm pores and a 60:1 L/d ratio have been ALD functionalized in a 20 cm × 20 cm square format. The substrates are mechanically and thermally (700˚C softening point) durable, and maintain excellent flatness during fabrication. We have implemented an imaging detector with a cross delay line readout[17] in order to assist in optimizing the ALD process. This system is capable of 50 µm FWHM spatial

resolution and event rates in excess of 1 MHz. The images, gain maps, and pulse amplitude distributions obtained during testing are essential in optimizing the ALD process.

Current 400 cm^2 ALD MCPs can be produced with similar gain characteristics to those achieved with the 33 mm round ALD MCPs. The absolute gain for a single plate is ~10^3 at 900 V (Fig. 14). The pulse amplitude distribution (Fig. 15) for UV light (185 nm) is consistent with previously published results[15]. The distribution is broader than that of 33 mm round ALD MCPs because of the larger gain variations found in the larger MCPs. Radioactive beta decay found throughout the bulk of the MCP glass dominates the background and has a negative exponential shape (Fig. 15).

Accumulating events using a 185 nm pen-ray lamp produces images of the MCP stack. The coarseness of the anode can be seen in the patterning of the image (Fig. 22). The initial gain map is very uniform over the whole 20 cm (Fig. 16 & 17). However, when an electrode is applied the gain became nonuniform (Fig. 18 & 19). The new gain map is very peaked in the center and low near the edges. We believe this is a result of the different depth of electrode deposition from the MCP center to the edge. The electrode is applied at 45˚ to the pores at the center of the plate. Because of the size of the MCP, the deposition angle is different at the edges and therefore metal is deposited deeper into the pores. The deeper deposition means there is a shorter acceleration region and lower gain. To reduce this effect, the deposition chamber has been changed so the source is at ~60˚ to the center pores. Figure 20 shows the difference between the two deposition setups.

Improvements have been made in the intrinsic background of 20 cm ALD MCPs. With such a large area (400 cm^2), it is difficult to keep the entire surface clear of debris. Any debris on the surface will create "warm spots" in the background image. It has been shown[18] that MCPs can be made without this problem and maintain low uniform background rates (~0.075 events cm^{-2} sec^{-1}). To date, the best background we have achieved with a 20 cm MCP has been ~0.04 events cm^{-2} sec^{-1} (Fig. 21) which is very close to the intrinsic Muon detection rate

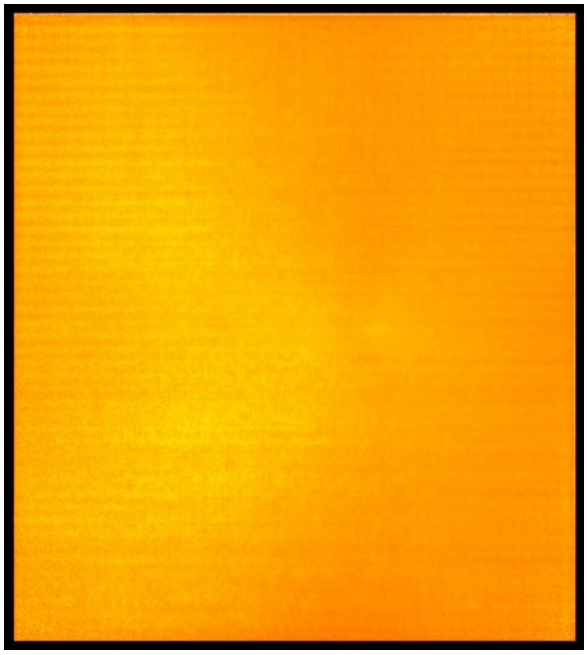

Fig. 16: Gain characteristics for a 20 cm MCP. Al_2O_3 ALD 20µm pore, 60:1 L/d borosilicate MCP. The gain is similar for both sides of the plate.

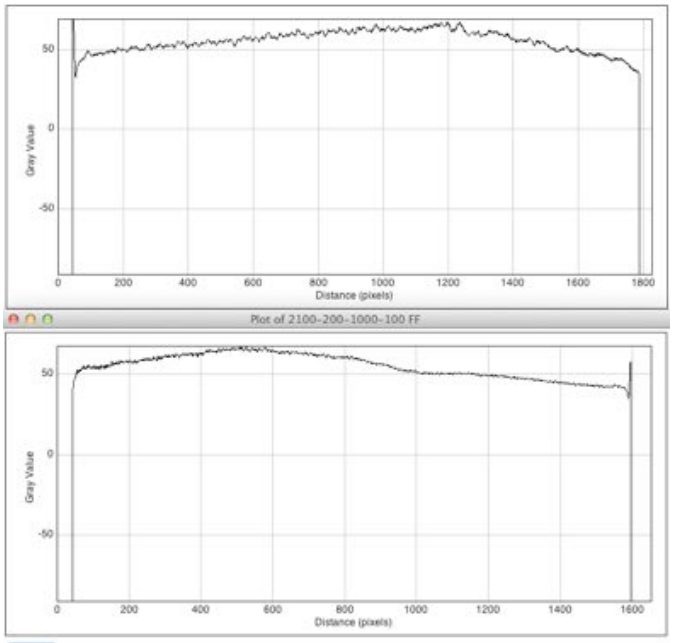

Fig. 17: Overall gain histograms for the image in Fig. 16. Variations are modest, given the large MCP area.

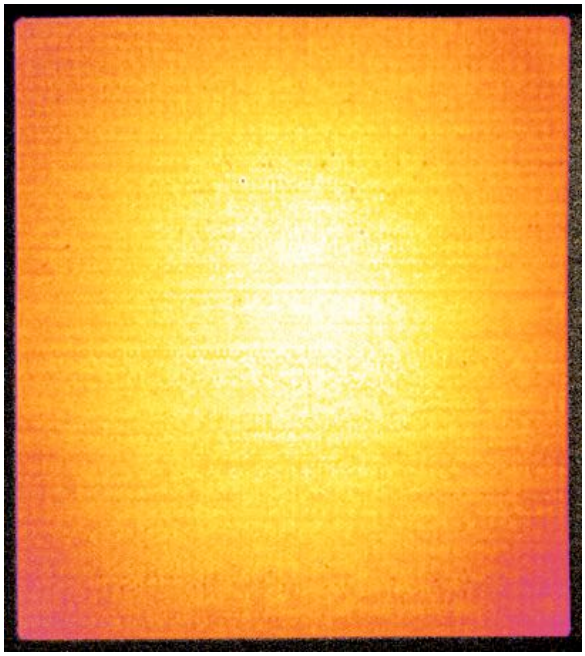

Fig. 18: Gain characteristics for a 20 cm MCP. Al_2O_3 ALD 20µm pore, 60:1 L/d borosilicate MCP. NiCr layer applied to both sides of the MCP pair.

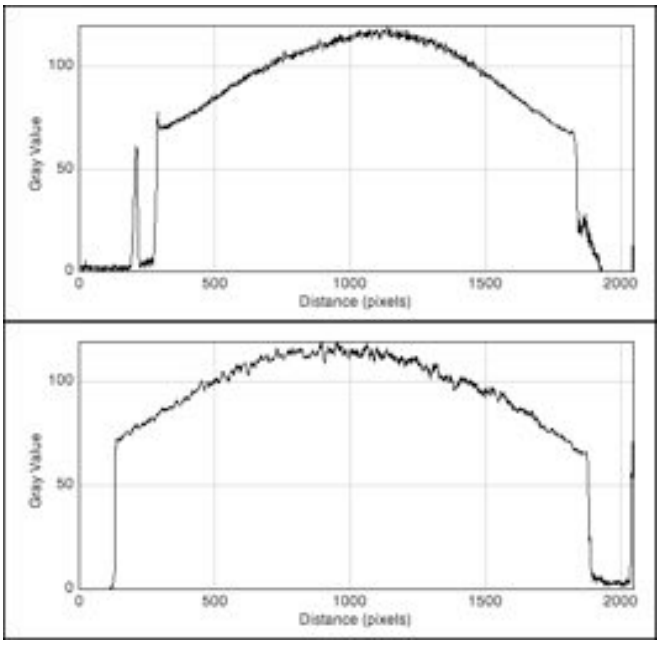

Fig. 19: Overall gain histograms for the image in Fig. 18. Gain is vary peaked in the center after the NiCr electrode deposition.

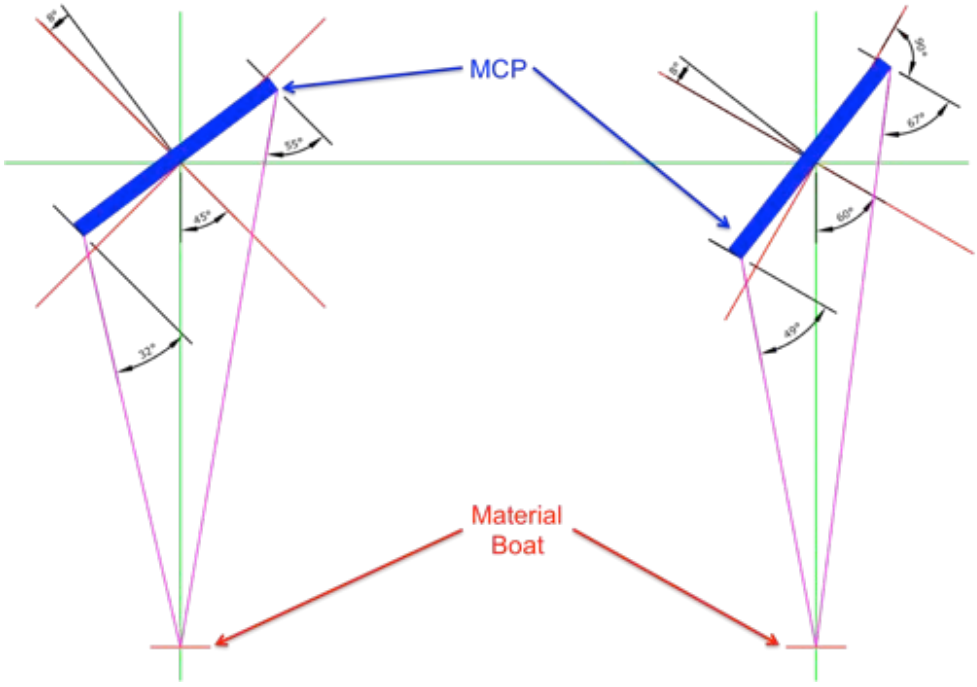

Fig. 20: Diagram of the electrode deposition. The material boat is heated to evaporate NiCr. The evaporation is line of sight and the MCP is rotated about the pores (8˚ bias) to increase uniformity. The size of the MCP causes the edges to have smaller deposition angles and therefore deeper

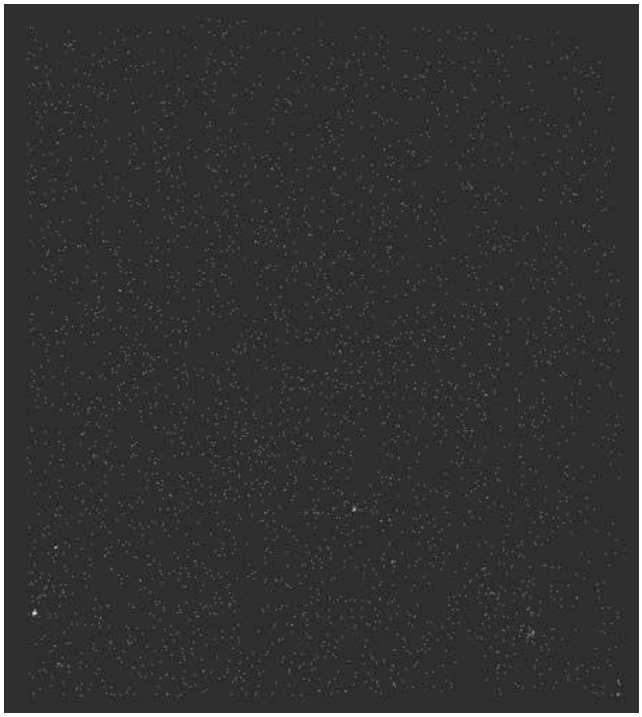

Fig. 21: Background Image. 20 cm square, 8°bias, 60:1 L/d ALD borosilicate MCP pair, Total Rate ~ 0.17 counts cm^{-2} sec^{-1}. Rate without hotspots <0.04 counts cm^{-2} sec^{-1}

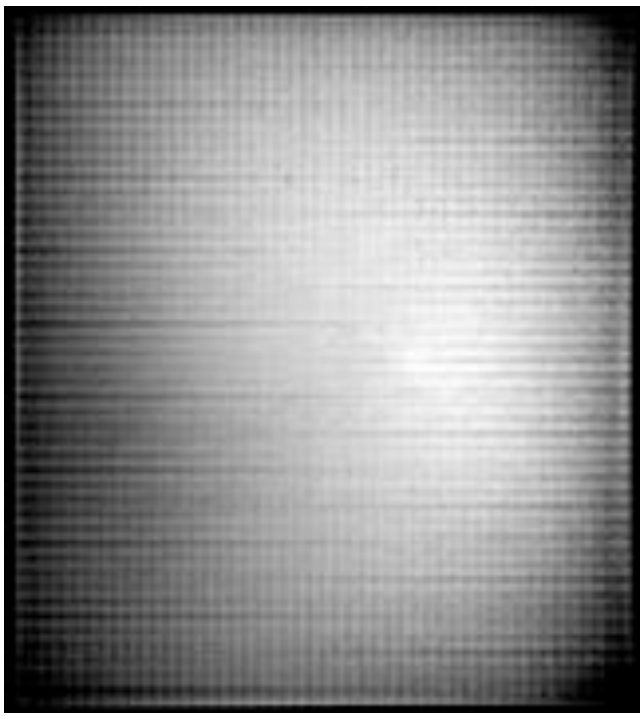

Fig. 22: Integrated image using 185 nm illumination for a pair of 200 mm square ALD MCPs (20 µm pore, borosilicate, 60:1 L/d, 8° bias). Inter-MCP 0.7 mm gap with 200v bias.

ACKNOWLEDGEMENTS

We wish to thank J. Hull, J. Tedesco, and S. Jelinsky for their contributions to this work. This work was supported by under NASA grants NNX11AD54G and NNX14AD34G, and DOE grant 005099.

REFERENCES

[1] Siegmund, O.H.W., Vallerga, J.V., Welsh, B., McPhate, J., Tremsin, A., "High speed optical imaging photon counting microchannel plate detectors for astronomical and space sensing applications," Proc. of the Advanced Maui Optical and Space Surveillance Technologies Conference, 90 (2009).

[2] Siegmund, O.H.W., Vallerga, J., Jelinsky, P., Michalet, X., Weiss, S., "Cross Delay Line Detectors for High Time Resolution Astronomical Polarimetry and Biological Fluorescence Imaging," Proc. IEEE Nuclear Science Symposium, 448-452 (2005).

[3] Tremsin, A.S., Lebedev, G.V., Siegmund, O.H.W., Vallerga, J.V., McPhate, J.B., Hussain, Z., "High resolution detection system for time of flight electron spectrometry," Nucl. Instr. Meth. **A582,** 172-174 (2007).

[4] Siegmund, O.H.W., Welsh, B.Y., Vallerga, J.V., Tremsin, A.S., McPhate, J.B., "High-performance microchannel plate imaging photon counters for spaceborne sensing," Proc. SPIE **6220**, (2006).

[5] Tremsin, A.S., Siegmund, O.H.W., Vallerga, J.V., Hull, J., "Cross Strip Readouts for Photon Counting Detectors with High Spatial and Temporal Resolution," IEEE Trans. Nucl. Sci. **51(N4),** 1707-1711 (2004).

[6] Siegmund, O. H. W., Jelinsky, P., Jelinsky, S., Stock, J., Hull, J., Doliber, D., Zaninovich, J., Tremsin, A., Kromer, K.S., "High resolution cross delay line detectors for the GALEX mission," *Proc. SPIE* **3765**, 429-440 (1999).

[7] Siegmund, O.H.W., [Methods of Vacuum Ultraviolet Physics 2nd edition, Chapter III], Academic Press, (1998).

[8] Lampton, M., "The microchannel image intensifier," Scientific American **245**, 62-71 (1981).

[9] Siegmund, O.H.W., Vallerga, J., Tremsin, A., "Characterizations of microchannel plate quantum efficiency," *Proc.* SPIE. **5898**, 58980H (2005).
[10] Frisch, H.J., "The development of large-area detectors with space and time resolution," Advances in Neutrino Technology workshop, (2009).
[11] Ritala, M., Leskelä, M.. "Atomic layer epitaxy - a valuable tool for nanotechnology?," Nanotechnology 10:1, 19 (1999)
[12] Siegmund, O.H.W., McPhate, J.B., Jelinsky, S.R., Vallerga, J.V., Tremsin, A.S., Hemphill, R., Frisch, H.J., Wagner, R.G., Elam, J., Mane, A., "Large area microchannel plate imaging event counting detectors with sub-nanosecond timing," IEEE. Trans. Nucl. Sci. 60(2), 923-931 (2013)
[13] Siegmund, O.H.W., Gummin, M.A., Stock, J., Marsh, D., "Microchannel plate imaging detectors for the ultraviolet," Proc. of an ESA Symposium on Photon Detectors for Space Instrumentation SP-356, (1992).
[14] Wisa, J.L., "Microchannel plate detectors," Nucl. Instr. Meth. 162**,** 587-601 (1979).
[15] Siegmund, O. H. W., Richner, N., Gunjala, G., McPhate, J. B., Tremsin, A., Frisch, H. J., Elam, J., Mane, A., Wagner, R., "Performance characteristics of atomic layer functionalized microchannel plates," Proc. of SPIE 8859, 88590Y (2013).
[16] Siegmund, O.H.W., "Preconditioning of microchannel plate stacks," *Proc. SPIE* 1072, 111-118 (1989).
[17] Siegmund, O.H.W., Vallerga, J.V., Tremsin, A.S., McPhate, J., Michalet, X., Weiss, S., Frisch, H.J., Wagner, R.G., Mane, A., Elam, J., Varner, G., "Large Area and High Efficiency Photon Counting Imaging Detectors with High Time and Spatial Resolution for Night Time Sensing and Astronomy," Proc. of the Advanced Maui Optical and Space Surveillance Technologies Conference, (2012)
[18] Siegmund, O. H. W., McPhate, J., Frisch, H., Elam, J., Mane, A., Wagner, R., Varner, G., "Large Area Flat Panel Imaging Detectors for Astronomy and Night Time Sensing," Proc. of the Advanced Maui Optical and Space Surveillance Technologies Conference, (2013).